

Standing Spin Waves in an Antiferromagnetic Molecular Cr₆ Horseshoe

S. T. OCHSENBEIN^{1 (a)}, O. WALDMANN¹, A. SIEBER¹, G. CARVER¹, R. BIRCHER¹, H. U. GÜDEL¹, R. S. G. DAVIES², G. A. TIMCO², R. E. P. WINPENNY², H. MUTKA³ and F. FERNANDEZ-ALONSO⁴

¹ *Department of Chemistry and Biochemistry, University of Bern, Freiestrasse 3, CH-3000 Bern 9, Switzerland*

² *Department of Chemistry, The University of Manchester, Oxford Road, Manchester M13 9PL, UK*

³ *Institut Laue-Langevin, 6 Rue Jules Horowitz, BP 156-38042, Grenoble Cedex 9, France*

⁴ *ISIS Facility, CCLRC Rutherford Appleton Laboratory, Didcot OX11 0QX, UK*

PACS 75.10.Jm – quantized spin models
PACS 33.15.Kr – magnetic moments and susceptibility of molecules
PACS 78.70.Nx – neutron inelastic scattering

Abstract. - The antiferromagnetic molecular finite chain Cr₆ was studied by inelastic neutron scattering. The observed magnetic excitations at 2.6 and 4.3 meV correspond, due to the open boundaries of a finite chain, to standing spin waves. The determined energy spectrum revealed an essentially classical spin structure. Hence, various spin-wave theories were investigated in order to assess their potential for describing the elementary excitations of finite spin systems.

Since the discovery of quantum tunneling of the magnetization in the molecules Mn₁₂ and Fe₈, the interest in molecular nanomagnets has soared [1]. Most of these molecules are characterized by dominant nearest-neighbor Heisenberg exchange interactions between the magnetic metal centers within a molecule, and additional weaker magnetic anisotropic terms (such as on-site anisotropy, dipole-dipole interactions, etc.). In these clusters, the nature of the ground state and elementary spin excitations is hence determined by the Heisenberg interactions. For a proper description of their magnetism it is thus of fundamental importance to understand the general question, what spin ground states and excitations may emerge from Heisenberg interactions on finite spin lattices (where finite is to be understood as to mean a few ten spin centers at most).

In this context, the antiferromagnetic rings and the Keplerate molecule Fe₃₀ have become prototypical examples [2–6]. Their low-lying energy spectrum exhibits a remarkable structure: In an energy vs total spin S representation it consists of a set of rotational bands whose energies increase as $E(S) \propto S(S+1)$ [7–10]. Physically, the lowest rotational band, the L band, reflects the rotational degree of freedom of the Néel-like antiferromagnetic ground state;

the higher rotational bands, collectively called E band, correspond to the (discrete) antiferromagnetic spin-wave excitations. For the case of the antiferromagnetic rings, this picture of the excitations has been confirmed experimentally in much detail [11], and also for Fe₃₀ evidence is strong [12]. Interestingly, the rotational band structure is found in other finite spin lattices, too, and is generic in this sense. Its emergence is correlated to a basically classical spin structure [8, 10, 11].

So far, most of the understanding of the elementary excitations in Heisenberg spin clusters was inferred from exact numerical diagonalization studies, which are obviously limited to systems with few spin sites. The classical spin structure identified in the above systems, however, suggests to consider approaches such as spin-wave theories (SWTs), which are standard in 3D systems, and have been demonstrated to be very capable also in 2D and 1D systems [13]. As a great advantage SWTs would allow one to treat much larger spin clusters, and exploring their applicability to molecular nanomagnets is hence of high interest, but no systematic study has emerged yet. Linear and modified SWTs were recently applied to Mn₁₂ and Fe₃₀ [14–16], with no general conclusions.

The examples of the antiferromagnetic rings, Fe₃₀, or Mn₁₂, exhibit relatively high symmetry and periodic boundary conditions. In this work, finite antiferromag-

^(a)Present address: Department of Chemistry, University of Washington, Seattle, WA 98195-1700, USA

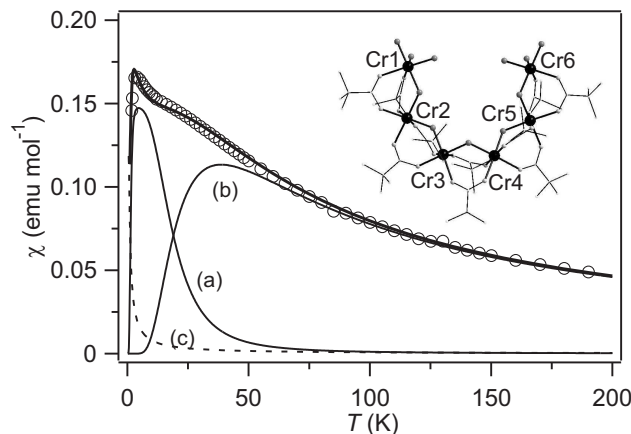


Fig. 1: Magnetic susceptibility vs temperature, $\chi(T)$, of Cr_6 . Open dots: data; thick line: calculated $\chi(T)$ as discussed in the text; thin lines: contributions from (a) the L -band states, (b) the remaining states, and (c) an impurity. The inset shows the molecular structure of the $[\text{Cr}_6\text{F}_{11}(\text{O}_2\text{CCMe}_3)_{10}(\text{H}_2\text{O})]^{3-}$ anion in Cr_6 .

netic Heisenberg chains, as described by the spin Hamiltonian

$$\mathcal{H} = -J \sum_{i=1}^{N-1} \mathbf{S}_i \cdot \mathbf{S}_{i+1}, \quad (1)$$

are considered ($J < 0$ is the coupling constant, N is the number of spin centers with spin length S_i). Finite antiferromagnetic chains were studied extensively before, for examples see Ref. [17]. Experimentally they were realized by intercepting infinite chains with non-magnetic dopants. This, however, yields a distribution of chain lengths, preventing observation of, e.g., individual spin-wave excitations [17]. The molecular compound $[\text{Pr}_2\text{NH}_2]_3[\text{Cr}_6\text{F}_{11}(\text{O}_2\text{CCMe}_3)_{10}(\text{H}_2\text{O})]$ (or Cr_6 in short) [18], in contrast, epitomizes a perfect finite chain: The anion of Cr_6 consists of six spin-3/2 Cr^{3+} ions forming a horseshoe structure, see fig. 1 [19], and the generic finite-chain Hamiltonian eq. (1) is the obvious magnetic model (with $N = 6$, $S_i = 3/2$). All molecules in a sample are identical, thus resolving the problem of the chain-length distribution, such that the Cr_6 compound provides unprecedented opportunities for the experimental study of the excitations in finite antiferromagnetic chains.

The spin excitations in finite chains show similarities to rings, but also differences. In particular, due to the open boundaries, the spin-wave excitations correspond to standing spin waves, as opposed to running waves in rings. In this work, we used inelastic neutron scattering (INS) to study the magnetic excitations in Cr_6 experimentally, and hence to observe the standing spin waves in a finite antiferromagnetic 1D system for the first time. We also extended the rotational-band structure concept to finite antiferromagnetic chains, and performed various SWT calculations to compare with the exact quantum mechanical result in order to explore the usefulness of these approaches.

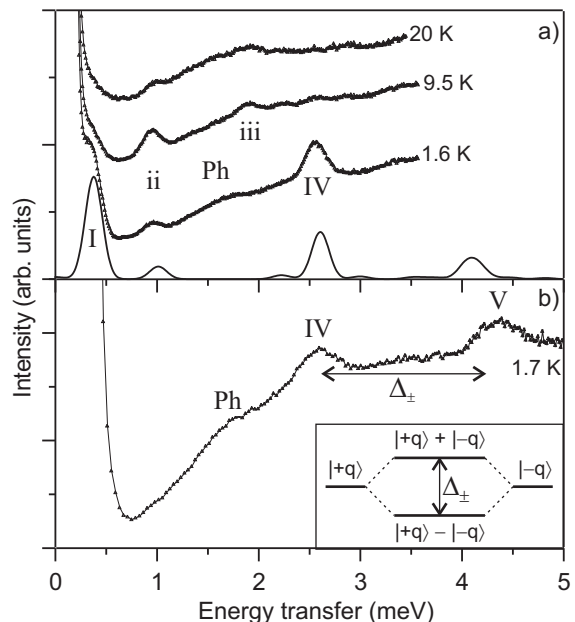


Fig. 2: Neutron energy-loss data of Cr_6 measured with (a) $\lambda = 3.8 \text{ \AA}$ and (b) $\lambda = 3.0 \text{ \AA}$. In (a) the curves are shifted for clarity. The solid line represents the calculated spectrum at low temperatures ($J = -1.27 \text{ meV}$, $T = 1.6 \text{ K}$, linewidth = 0.2 meV). Δ_{\pm} denotes the E -band splitting, schematically depicted in the inset.

A powder sample of undeuterated Cr_6 was synthesized as in [18]. The magnetic susceptibility was measured at a field of 0.1 T with a SQUID magnetometer (Quantum Design). INS experiments in the temperature range $1.5 - 20 \text{ K}$ were performed on the instruments IN5 (Institut Laue-Langevin, Grenoble, France), and IRIS (ISIS, Didcot, UK). The data treatment employed a correction for detector efficiency by a vanadium standard. The data shown in this work were obtained on IN5 with initial wavelengths of $\lambda = 3.0 \text{ \AA}$ and 3.8 \AA . The experimental resolution at the elastic line was 0.40 meV and 0.17 meV , respectively.

The magnetic susceptibility vs temperature, $\chi(T)$, of Cr_6 is shown in fig. 1. It exhibits a peak at 5 K and a shoulder at 35 K . Observation of such a behavior is unusual; a similar behavior has been reported previously only for the antiferromagnetic wheel Cr_8Ni [20]. The calculated susceptibility (thick solid line in fig. 1) was based on eq. (1) with $J = -1.27 \text{ meV}$ as found from INS (*vide infra*), $g = 1.96$ which is typical for Cr^{3+} , and a Curie-type contribution which accounts for a small amount of paramagnetic impurity ($C = 0.08 \text{ emu K mol}^{-1}$). The agreement is very good, given that g and C were the only adjustable parameters.

The INS data recorded on IN5 at various temperatures are shown in fig. 2. Six inelastic features at about 0.4 meV (I), 1.0 meV (ii), 1.7 meV (Ph), 1.9 meV (iii), 2.6 meV (IV), and 4.3 meV (V) are observed. The broad band Ph and the rising background are assigned to a non-magnetic

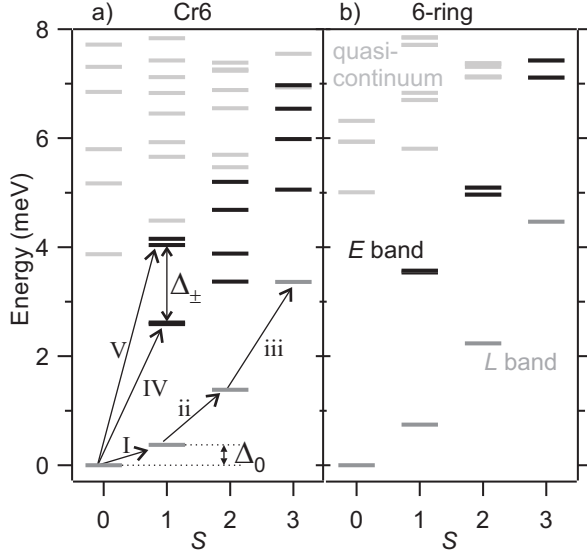


Fig. 3: Calculated energies vs total spin S for (a) Cr₆ with $J = -1.27$ meV and (b) a $N=6$ spin-3/2 ring with $J_{\text{ring}} = \frac{5}{6}J$. The lowest states for each $S \geq 0$ form the L band (dark gray levels), the 4 next-higher levels for each $S \geq 1$ the E band (black levels), and the remaining states the quasi-continuum (light gray levels).

origin (incoherent scattering of protons, phonons, internal rotations of methyl groups, etc.) [21]. The other, resolution-limited peaks are assigned to magnetic transitions. The temperature dependence of the 3.8 Å spectrum reveals that peaks I, IV, and V are cold transitions, while peaks ii and iii are hot transitions.

The INS spectra were simulated by numerically diagonalizing eq. (1) and calculating the intensities from the wavefunctions using the formulas of Ref. [22]. The solid line in fig. 2(a) represents the calculated spectrum for $J = -1.27$ meV. The agreement with experiment is very good, considering that the model includes only one free parameter (J) [23]. The calculated position of peak V at 4.1 meV is 5% too low, which indicates a weak variation of the exchange coupling constants along the chain [24]. These results demonstrate that the generic antiferromagnetic chain model eq. (1), while it does not describe Cr₆ perfectly, clearly provides a very good starting point for the discussion of the physical nature of the elementary excitations in Cr₆.

Figure 3(a) presents the calculated lowest energy levels vs S , with the observed transitions indicated by arrows. The three cold peaks I, IV and V correspond to transitions from the $S = 0$ ground state to the five lowest triplets (which will be identified below as the $S = 1$ states of the L and E bands, respectively). Peaks IV and V each consist of two transitions, which are too close to be resolved in the experiment. Peaks ii and iii originate from hot transitions within the L band, as indicated in fig. 3(a).

In the following, the low-temperature triplet excitations I, IV, and V in Cr₆ will be analyzed from two points of

view. First, Cr₆ is regarded as a hexanuclear antiferromagnetic ring with a missing bond (J_{61}) as a perturbation, i.e., the Hamiltonian is written as $\mathcal{H} = -J(\sum_{i=1}^5 \mathbf{S}_i \cdot \mathbf{S}_{i+1} + \mathbf{S}_6 \cdot \mathbf{S}_1) + \mathcal{V}$ with $\mathcal{V} = J\mathbf{S}_1 \cdot \mathbf{S}_6$. Second, various variants of SWT will be applied.

The situation in an antiferromagnetic $N=6$ spin-3/2 ring is briefly recalled [10]. The energy spectrum for $J_{\text{ring}} = 5/6J$ is depicted in fig. 3(b) (the factor 5/6 adjusts for the different number of antiferromagnetic bonds in the chain and ring). It is characterized by a L band, an E band, and the quasi-continuum. The separation of the spectrum into L/E bands and a quasi-continuum originates from the fact, that the INS intensity of transitions from states of the L band to states of the quasi-continuum is essentially zero, i.e., all intensity goes into transitions within the space of the L and E bands. Importantly, these properties are intimately connected to a classical spin structure [8, 10].

Comparing figs. 3(a) and 3(b) reveals that the concept of a L band, E band, and quasi-continuum is still useful for the finite chain. This is obvious for the L band, though not for the E band. However, a careful inspection of the transition matrix elements shows that almost all low-temperature intensity goes into transitions to the states displayed in dark gray and black in fig. 3(a). For instance, transitions I, IV, and V account for 97.4% of the total intensity. Thus, although the states which form the E band in Cr₆ are not easily recognized from the energy spectrum, they are clearly identified by the transition intensities.

For a finite antiferromagnetic chain, as compared to an antiferromagnetic ring, two differences are noted. First, the gap between the ground state and the lowest triplet Δ_0 (singlet-triplet gap) is rather small. This explains the peak and shoulder in $\chi(T)$. Figure 1 disentangles the contributions to $\chi(T)$ from (a) the L band (which is responsible for the peak at about 5 K), (b) all other states (which produces the shoulder at about 35 K), and (c) the impurity. As the L band is governed by Δ_0 , the observation of a peak separated from a shoulder directly reflects a comparatively smaller Δ_0 : In the antiferromagnetic rings the L -band contribution (a) is shifted towards higher temperatures and hence less separated from contribution (b), such that only a broad maximum is observed in $\chi(T)$ [2]. A second important difference is the splitting of the E band into two subgroups in the $N=6$ antiferromagnetic chain [from fig. 3(a) this is obvious for the triplets, but less so for $S > 1$]. The splitting of the E band is a direct consequence of the different boundary conditions for the spin waves in chains and rings.

Considering a finite antiferromagnetic chain as a ring with a missing bond provides an intuitive picture. The cyclic symmetry of a ring implies a shift quantum number $q = (r - \frac{N}{2})\frac{2\pi}{N}$, with $r = 1, 2, \dots, N$ and $\hat{T}|q\rangle = e^{-iq}|q\rangle$ (\hat{T} is the shift operator). The ground state belongs to $q = 0$, the triplet of the L band to $q = \pi$, and the triplets

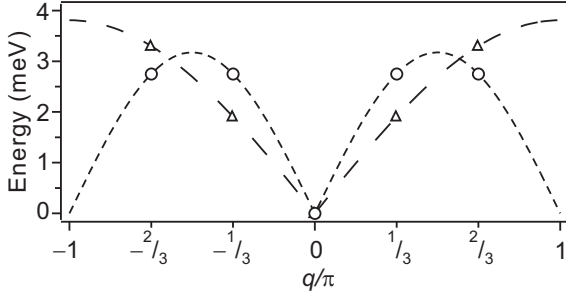


Fig. 4: Spin-wave dispersions vs q obtained from linear SWT for chains with periodic (dotted line) and open (dashed line) boundary conditions. Symbols indicate the predicted energies for Cr_6 (Δ) and a $N=6$ ring (\circ).

of the E band to $q = \pm\frac{1}{3}\pi, \pm\frac{2}{3}\pi$ for a $N = 6$ ring. In the ring, the states with q and $-q$ are degenerate by symmetry, but in Cr_6 the perturbation of the missing bond produces a splitting in first order since $\langle -q|\mathcal{V}|+q\rangle \neq 0$. Accordingly, the wavefunctions are no longer eigenstates of q (running waves), they are given by the symmetric and antisymmetric mixtures

$$|q\rangle_{\pm} = | +q\rangle \pm | -q\rangle, \quad (2)$$

as depicted in the inset of fig. 2. These wavefunctions can be considered as the cosine and sine components built from $| -q\rangle$ and $| +q\rangle$, in analogy to $e^{-iq} \pm e^{iq}$, and hence represent standing waves. In Cr_6 the splitting between them is given by $\Delta_{\pm} = 2|\langle -\frac{\pi}{3}|\mathcal{V}|\frac{\pi}{3}\rangle| = 2|\langle -\frac{2\pi}{3}|\mathcal{V}|\frac{2\pi}{3}\rangle|$, and the E -band triplets organize into two groups separated by Δ_{\pm} , see fig. 3a (the small splitting of the two states within one group, which increases with S , is a higher-order effect). Obviously, the observation of peaks IV and V in Cr_6 , fig. 2, directly reflects the splitting Δ_{\pm} due to the formation of the $|q\rangle_{\pm}$ states, i.e., the observation of standing spin waves in a finite antiferromagnetic chain.

Another simple rational for the E -band splitting is obtained from linear SWT. The dispersion relations for an infinite antiferromagnetic chain with periodic or open boundary conditions (BC), respectively, are [7, 25]

$$\begin{aligned} \text{periodic BC: } \hbar\omega_q &= 2S_i|J_{ring}\sin(q)|, \\ \text{open BC: } \hbar\omega_q &= 2S_i|J\sin(q/2)|. \end{aligned} \quad (3)$$

They are displayed in fig. 4. In a finite spin cluster, however, only the discrete waves with the q 's restricted to the above values are possible. The spin-wave energies for a $N = 6$ system are indicated in fig. 4 by open symbols. For an antiferromagnetic $N=6$ ring, four almost degenerate spin waves are predicted, while for an antiferromagnetic $N=6$ chain the spin waves are organized into two groups, exactly as was just discussed.

As pointed out already in the above, the rotational-band structure implies a classical spin structure in the L and E bands. This suggests to compare the results of various semi-classical theories (the details of our calcula-

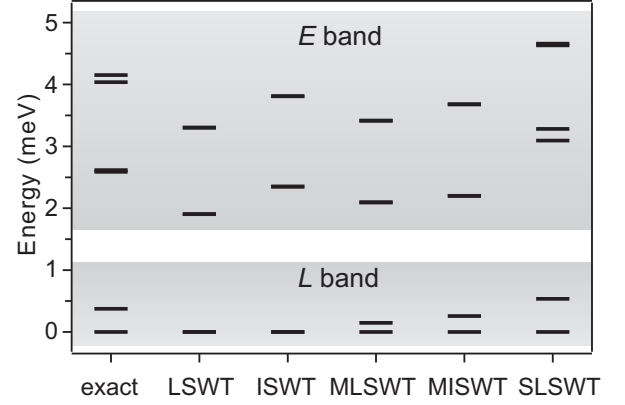


Fig. 5: Calculated levels for an antiferromagnetic $N = 6$ spin- $3/2$ chain comparing the exact result and the results of the SWT calculations for $J = -1.27$ meV (LSWT = linear SWT, ISWT = interacting SWT, MLSWT = modified-linear SWT, MISWT = modified-interacting SWT, SLSWT = spin-level SWT). The shaded areas highlight the two lowest L -band states and the E -band triplets.

tions will be reported elsewhere). The most widely recognized semi-classical theory in magnetism is SWT. Here, one starts from the classical ground state (which in the present case is the Néel state with all spins oriented up or down) and accounts for quantum fluctuations by replacing the spin operators by Holstein-Primakoff or Dyson-Maleev bosons [13]. This yields a boson Hamiltonian \mathcal{H}_B in real space, which is the appropriate starting point for finite spin systems as pointed out in Ref. [16].

In linear SWT, the boson Hamiltonian \mathcal{H}_B is truncated to terms quadratic in the boson operators. The spin-wave energies are then obtained from a Bogoliubov diagonalization (in this work, the Bogoliubov diagonalization was performed numerically for all SWT calculations). Interacting SWT additionally includes the effects of 4th-order boson terms [13].

A serious drawback of these kind of theories is that they start from the assumption of an ordered, symmetry-broken ground state, which for finite clusters is obviously incorrect. As a result they are unable to reproduce the singlet-triplet gap, which is characteristic for finite spin systems. These theories hence miss the experimentally observed peak I. Modified SWTs have become popular to correct for this deficiency [16, 26]. Here, the rotational invariance is restored by imposing the conditions $\langle S_i^z \rangle = 0$ of zero on-site magnetization via Lagrange multipliers. Modified-linear SWT goes up to quadratic boson terms, and modified-interacting SWT up to 4th-order boson terms.

Finally, a further approach is suggested. For antiferromagnetic rings (and similarly for other antiferromagnetic clusters such as Fe_{30}) the rotational-band structure implies approximating the wavefunctions of the L and E bands by the spin levels $|\alpha S_A S_B S_M\rangle$, where S_A and S_B are the total spins on each of the two antifer-

romagnetic sublattices A and B (α denotes intermediate spin quantum numbers) [6, 8, 10]. The L band is obtained for $S_A = S_B = S_i N/2$, while the space of the E band is spanned by the spin levels with $S_A = S_i N/2$, $S_B = S_i N/2 - 1$, and vice versa [10]. This suggests to diagonalize \mathcal{H} in the space of the spin levels $|\alpha S_A S_B S M\rangle$ with the above values for S_A , S_B . This approach is called spin-level SWT.

The results obtained for Cr₆ with all these techniques are shown in fig. 5 and compared to the exact values obtained numerically by exact diagonalization. Some general trends can be observed (which have been confirmed by studies on more spin clusters). First the E band is discussed. For infinite spin systems the experience is that linear SWT underestimates energies, while interacting SWT often yields very good results [13]. For Cr₆ a similar trend is observed. The linear SWT results are well below the exact energies, while interacting SWT comes rather close, within 8% accuracy for Cr₆. The results of the modified SWTs show a similar trend, i.e. modified-interacting SWT yields a better agreement with the exact result than modified-linear SWT, although not quite as good as interacting SWT. In contrast to these (bosonic) SWTs, spin-level SWT overestimates the spin-wave energies, by about 30% for Cr₆. As mentioned before, the modified SWTs yield a finite singlet-triplet gap Δ_0 as does the spin-level SWT. Δ_0 from modified-interacting SWT turns out 30% smaller than the exact result, while the spin-level SWT calculates it 50% too large (the performance of modified-linear SWT is even worse).

Hence, we observe that the bosonic SWTs underestimate the energies while the spin-level SWT overestimates them. The interacting SWT yields the best results for the spin-wave energies, but is not able to reproduce a non-zero singlet-triplet gap (by construction). The modified-interacting and spin-level SWTs both yield a non-zero value for the singlet-triplet gap Δ_0 , but the overall accuracy is modest, with no clear advantage for one or the other. A conceptional advantage of spin-level SWT though is that it is rotationally invariant, and that it can be naturally extended to systems with, e.g., three sublattices such as Fe₃₀, where the non-collinear spin structures require special attention in the interacting SWTs.

In conclusion, we have observed the standing spin-wave excitations in the molecular antiferromagnetic finite-chain compound Cr₆ experimentally. We systematically investigated the capabilities of various SWTs in describing the elementary excitations of finite Heisenberg spin clusters. In our opinion, such investigations are of great value with regard to molecular nanomagnets where exact results are not accessible. The extendability of the rotational-band concept to spin systems such as finite antiferromagnetic chains underpins a certain generality.

We thank O. Cépas and T. Ziman for many useful dis-

cussions. Financial support by EC-RTN-QUEMOLNA, contract n° MRTN-CT-2003-504880, and the Swiss National Science Foundation is acknowledged.

REFERENCES

- [1] GATTESCHI D. and SESSOLI R., *Angew. Chem. Int. Ed.*, **42** (2003) 268.
- [2] TAFT K. L., DELFS C. D., PAPAETHYMIU G. C., FONER S., GATTESCHI D. and LIPPARD S. J., *J. Am. Chem. Soc.*, **116** (1994) 823.
- [3] GATTESCHI D., CANESCHI A., PARDI L. and SESSOLI R., *Science*, **265** (1994) 1054.
- [4] WALDMANN O., *Coordin. Chem. Rev.*, **249** (2005) 2550.
- [5] MÜLLER A., LUBAN M., SCHRÖDER C., MODLER R., KÖGERLER P., AXENOVICH M., SCHNACK J., CANFIELD P. C., BUDKO S. and HARRISON N., *ChemPhysChem.*, **2** (2001) 517.
- [6] SCHNACK J., LUBAN M. and MODLER R., *Europhys. Lett.*, **56** (2001) 863.
- [7] ANDERSON P. W., *Phys. Rev.*, **86** (1952) 694.
- [8] BERNU B. *et al.*, *Phys. Rev. Lett.*, **69** (1992) 2590; LE-CHEMINANT P. *et al.*, *Phys. Rev. B*, **52** (1995) 6647.
- [9] SCHNACK J. and LUBAN M., *Phys. Rev. B*, **63** (2000) 014418.
- [10] WALDMANN O., *Phys. Rev. B*, **65** (2002) 024424.
- [11] WALDMANN O., GUIDI T., CARRETTA S., MONDELLI C. and DEARDEN A. L., *Phys. Rev. Lett.*, **91** (2003) 237202.
- [12] GARLEA V. O., NAGLER S. E., ZARESTKY J. L., STASSIS C., VAKNIN D., KÖGERLER P., MCMORROW D. F., NIEDERMAYER C., TENNANT D. A., LAKE B., QIU Y., EXLER M., SCHNACK J. and LUBAN M., *Phys. Rev. B*, **73** (2006) 024414 and references therein. WALDMANN O., *Phys. Rev. B*, **75** (2007) 012415.
- [13] IVANOV N. B. and SEN D., *Lecture Notes in Physics*, **645** (2004) 195.
- [14] YAMAMOTO S. and NAKANISHI T., *Phys. Rev. Lett.*, **89** (2002) 157603.
- [15] CHABOUSSANT G., SIEBER A., OCHSENBEIN S., GÜDEL H.-U., MURRIE M., HONECKER A., FUKUSHIMA N. and NORMAND B., *Phys. Rev. B*, **70** (2004) 104422.
- [16] CÉPAS O. and ZIMAN T., *Prog. Theo. Phys. Suppl.*, **159** (2005) 280.
- [17] HAGIWARA M., KATSUMATA K., AFFLECK I., HALPERIN B. I. and RENARD J. P., *Phys. Rev. Lett.*, **65** (1990) 3181; DITUSA J. F., CHEONG S. W., PARK J. H., AEPPLI G., BROHOLM C. and CHEN C. T., *Phys. Rev. Lett.*, **73** (1994) 1857; FUJIWARA N., YASKUOKA H., ISOBE M. and UEDA Y., *Phys. Rev. B*, **58** (1998) 11134; LOU J., QIN S., NG T.-K., SU Z. and AFFLECK I., *Phys. Rev. B*, **62** (2000) 3786; BOGANI L., CANESCHI A., FEDI M., GATTESCHI D., MASSI M., NOVAK M. A., PINI G. M., RETTORI A., SESSOLI R. and VINDIGINI A., *Phys. Rev. Lett.*, **92** (2004) 207204; PARKINSON J. B., *J. Phys.: Condens. Matter*, **16** (2004) S5233; FURRER A. and GÜDEL H.-U., *Eur. Phys. J. B*, **16** (2000) 81.
- [18] LARSEN F. K., OVERGAARD J., PARSONS S., RENTSCHLER E., SMITH A. A., TIMCO G. A. and WINPENNY R. E. P., *Angew. Chem. Int. Ed.*, **42** (2003) 5978.

- [19] The anions in Cr₆ are arranged in pairs separated by six [nPr₂NH₂]⁺ cations; nPr stands for n-propyl.
- [20] CADOR O., GATTESCHI D., SESSOLI R., LARSEN F. K., OVERGAARD J., BARRA A.-L., TEAT S. J., TIMCO G. A. and WINPENNY R. E. P., *Angew. Chem. Int. Ed.*, **43** (2004) 5196.
- [21] The non-magnetic origin was shown by correcting the data by a Bose-population factor for phonons and comparing different temperatures.
- [22] WALDMANN O., *Phys. Rev. B*, **68** (2003) 174406.
- [23] The three very weak peaks appearing in the calculated spectrum at 2.2, 3.0 and 3.5 meV stem from transitions too weak to be observed experimentally, and hence are not labeled.
- [24] $J_{12} = J_{56} = -1.1$ meV, $J_{23} = J_{34} = J_{45} = -1.4$ meV. The Cr ions Cr1 and Cr6 have a different coordination sphere than the Cr ions Cr2 – Cr5. The coordination spheres affect the nearest-neighbor exchange interactions, hence J_{12} and J_{56} are expected to be slightly different from J_{23} , J_{34} , and J_{45} (more details will be reported elsewhere).
- [25] MCGURN A. R. and THORPE M. F., *J. Phys. C: Solid State Phys.*, **16** (1983) 1255.
- [26] TAKAHASHI M., *Phys. Rev. Lett*, **58** (1987) 168; HIRSCH J. E. and TANG S., *Phys. Rev. B*, **40** (1989) 4769.